Climatic Change (2026) 179:110
https://doi.org/10.1007/s10584-026-04203-7

High resolution assessment of forest wind risk under historical and future climate conditions

Tommaso Baggio[1] · **Giorgia Fosser**[2] · **Tommaso Locatelli**[3] · **Emanuele Lingua**[1,4]

Received: 12 January 2026 / Accepted: 28 April 2026

Abstract
Windstorms are the principal cause of disturbance to European forests, and their frequency and magnitude are expected to increase by the end of the century due to climate change. Several studies have assessed the risk of forest damage from wind disturbances, but most were limited by the accuracy of forest vulnerability or by climate data, especially in complex terrain such as the Alps. In this study, we assessed and mapped forest wind risk at high resolution (20 × 20 m) under historical (1996–2005) and future (2090–2099, Representative Concentration Pathway 8.5) reference periods. The study takes advantage of high-resolution remotely sensed data to derive individual tree and stand characteristics for calculating forest vulnerability with ForestGALES, a hybrid mechanistic-empirical forest wind risk model. The investigation focuses on the impact of changes in wind intensities between the historical and the future scenarios on forest risk by fixing the same forest vulnerability map derived from a LiDAR survey acquired in 2019. Wind intensities were derived from an ensemble of high temporal and spatial resolution convection-permitting models. Combining these two datasets, we produced high resolution mapping of forest wind risk for an area in the Dolomites in North-east Italy. This study classifies the forest area into three levels of risk, and it quantitatively assesses the relative amount of growing stock at risk. Results for a case study forest area of 268 km^2 show that the growing stock at risk is equal to 8.5% and increasing to 10.0% under the historical and future reference periods, respectively. The risk maps clearly identified the areas at higher risk, mainly those composed of pure Norway spruce stands, providing fundamental insights for improving forest resistance to wind at the regional scale.

Keywords Forest disturbances · Convective permitting model · Windstorm · Risk mapping · Remote sensing

Extended author information available on the last page of the article

Published online: 08 May 2026

1 Introduction

Extreme meteorological events are responsible for direct and indirect impacts on forest stands (DeWalle et al. 2003). Due to climate change, the frequency and magnitude of such events are likely to increase, especially for some areas in Europe (Outten and Sobolowski 2021), potentially causing an increase in forest losses in the next decades (Seidl et al. 2017). Among the different sources of forest disturbances, windstorms are recognized as the leading cause of forest damage in Europe (Patacca et al. 2023). Therefore, both in current climate conditions and even more importantly under a climate change scenario, future projections of wind-related forest risk are essential for identifying the most critical geographical areas and consequently informing management strategies aimed at increasing forest resistance and resilience.

The concept of risk can be defined as the combination of vulnerability and frequency of occurrence of a certain event (Crozier and Glade 2005; Renn 2008). In the case of forest wind disturbances, risk assessment implies the estimation of the forest stand vulnerability to wind damage and the frequency-magnitude of windstorm events (Blennow and Olofsson 2008). Therefore, risk estimation requires integrating information on forest characteristics (used to derive its vulnerability) and climatic conditions for assessing windstorm magnitude. Given the relevance of location-specific factors (e.g., topography, microclimatic conditions, etc.) to the characteristics of both the hazard (extreme winds) and the vulnerability (typically, the critical wind speeds of damage) of a tree/forest system, wind risk is best computed and displayed spatially using digital maps. These are often the preferred medium for forest management and planning activities (Fassnacht et al. 2025).

For the calculation of forest wind vulnerability, different models have been developed to derive the Critical Wind Speed (CWS), that is the wind speed that would damage a given tree or a forest stand with certain characteristics (Gardiner et al. 2000). In recent years, significant advances have been made in the scientific understanding of the dynamics of wind damage and of the associated factors. Early wind damage models mainly relied on a statistical approach (Flesch and Wilson 1999). Successively, driven by the increasing scientific understanding of wind loading and damage dynamics, hybrid mechanistic models started to appear (Peltola et al. 1999). These models offer several advantages, including applicability to different geographic regions, silvicultural practices, and complex modelling frameworks. Such strengths are responsible for the popularity and wide range of applications of these models (Kamimura and Shiraishi 2007; Hale et al. 2015; Costa et al. 2023; Gardiner et al. 2024).

The most common examples of hybrid mechanistic models are ForestGALES (Hale et al. 2015; Quine et al. 2021), HWind (Peltola et al. 1999) and FOREOLE (Ancelin et al. 2004). Whilst differences exist between the formulation of these models, the CWS is typically calculated from the relationship between the resistive moment of a tree (independently for uprooting and stem breakage) and the force applied by the wind on the components of the tree (Peltola 2006). The input data of hybrid mechanistic models include tree and stand characteristics, together with a set of species-specific parameters. Studies highlighted that at the single tree level, tree height, diameter, crown extension, species, size/depth of the root system, and distance to the forest edge are the main characteristics influencing resistance to wind damage (Quine et al. 2021). At the stand level, factors affecting the wind resistance are the mean tree height, stand dominant height, mean stem diameter, mean tree taper, stand

density, the location and size of upwind forest gaps, and the degree of acclimation of the forest edges (Kamimura et al. 2017). While hybrid mechanistic models have been validated multiple times using different data sources (Gardiner et al. 2008, 2024; Hale et al. 2015), ensuring that the input data are as accurate and as representative of the tree/forests for which wind risk metrics are calculated remains paramount to minimize uncertainty in the model outputs (Locatelli et al. 2017). An important step forward was achieved by Baggio et al. (2026) where the authors developed a semiautomatic routing procedure to derive high-resolution spatially distributed CWS from LiDAR (Laser Imaging Detection And Ranging) data. This approach offers notable improvements in the identification of the most wind vulnerable forest areas, together with a significant reduction in the requirements for gathering field data to compute the wind risk metrics.

On the other hand, climatic data are the other fundamental component for mapping the wind risk in forests. The frequency-intensity relationship of wind speeds is essential to characterize the wind hazard and thus accurately quantify the risk level of a given forest area. This relationship can be derived from historical time series of wind data collected by meteorological stations. However, differently from other meteorological variables (precipitation, temperature, etc.), wind intensity and wind direction data are often less consistently recorded across stations, and available time series are frequently limited in length and spatial distribution (Rojas-Labanda et al. 2023). An alternative solution to obtain spatially distributed wind data is presented by climate models. In mountainous and hilly areas, orography plays a crucial role in affecting the wind intensity across different wind directions, and therefore its influence needs to be considered. In most cases, the orography decreases the wind intensity by sheltering some locations, but in other circumstances, wind intensity can be enhanced through the so-called "tunnel effect" that occurs when mountain valleys narrow along the same direction of the prevailing wind. In addition, complex turbulence patterns can develop on the leeway side of hills, promoting the development of areas of reverse wind flow and of highly turbulent areas (Kaimal and Finnigan 1994), a condition further exacerbated when mountains are heavily forested (Finnigan and Belcher 2004). Numeric solutions to model wind flow over moderate terrain are provided by linear airflow models such as WAsP (Wind Atlas Analysis and Application Program), which incorporates the influence of local topography, changes in aerodynamic roughness across the landscape, and the presence of obstacles (Mortensen et al. 1999). For more complex topography, the TOPEX index (TOPographic EXposure index) (Chapman 2000) likely represents a better alternative. TOPEX describes wind exposure using only a quantitative assessment of the horizontal inclination of the terrain over a fixed distance from each calculation point. Despite its simplicity, this index has been proven to be able to model the orographic effect on the wind intensity of the storm Vaia (Oct. 2018) in the Italian Alps, allowing back-casting of forest damage caused by the storm when combined with wind data from local meteorological stations (Costa et al. 2023).

The present study aims to develop and implement a novel methodology for mapping forest wind risk, adopting high-resolution data. The procedure is applied on a mountainous area in the Dolomites, Eastern Italian Alps, characterized by a heterogeneous forest cover and a complex orography. The proposed methodology integrates high-resolution forest wind vulnerability maps with km-scale climate data to generate detailed risk maps. The forest vulnerability map is derived from a LiDAR survey acquired in 2019 and is applied in both the historical and future scenarios. This approach underpins the study's objective, which is to isolate and assess the impact of climate change-driven changes in projected wind intensi-

ties on forest wind risk mapping. To achieve this, the study evaluates how climate change will impact wind intensities under the representative climate scenario (RCP) 8.5. For both historical and future scenarios, the study aims to quantitatively assess wind risk to forests in terms of forest areas and biomass volume at risk, providing fundamental and innovative insights into the impacts of climate change on the risk of wind damage.

2 Study area

The study area covers an extent of 477 km^2 within the Belluno province in the Eastern Italian Alps and geologically belongs to the dolomitic zone. It is located in the upper part of the Cordevole catchment, also named "Alto Agordino". The elevation ranges from 483 to 3343 m a.s.l. including the highest peak of the Dolomites, Marmolada. The morphology is characterized by a north-south valley, where the Cordevole torrent flows, with 5 secondary valleys (perpendicular to the main one) all located on the western side (Fig. 1). The slopes are quite steep with gradients mainly between 15 and 45°.

Forests cover 279 km^2, i.e. 58% of the total area. The predominant species in terms of area is Norway spruce (*Picea abies* (L.) Karst., 37.6%), followed by larch (*Larix decidua* Mill., 29.0%), beech (*Fagus sylvatica* L., 12.6%), other broadleaves (3.5%), and Scots pine (*Pinus sylvestris* L., 1.9%). At high altitude, there is a large presence of dwarf mountain pine (*Pinus mugo* T., 10.2%) and green alder (*Alnus alnobetula* (Ehrh.) K.Koch, 4.8%). Within these two latter types of forest cover, it is frequent to find single trees or small groups mainly

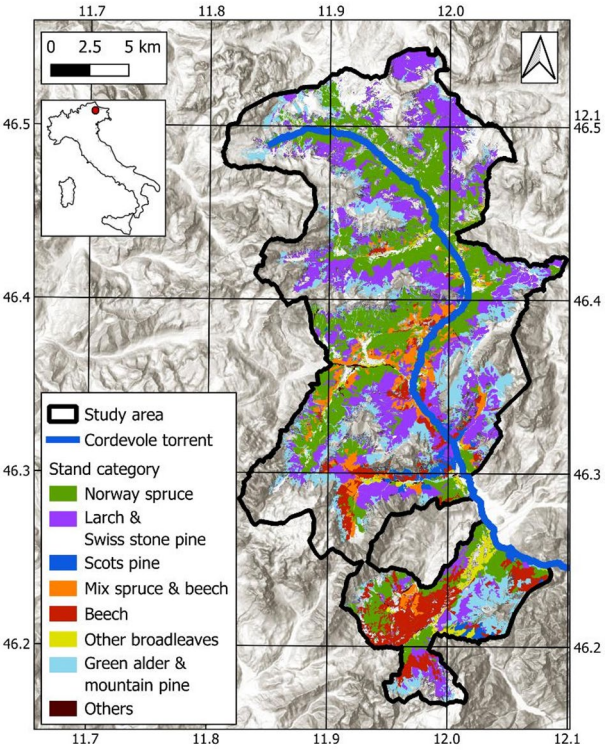

Fig. 1 Hillshade overview of the study area with the path of the Cordevole torrent and the forest stand category

of Norway spruce or, on some occasions, of larch. Larch is predominant at high altitudes near the tree line; as the elevation decreases, Norway spruce becomes the dominant species, particularly on north-facing slopes. On south-facing slopes at medium altitude, beech can form pure stands or can be found mixed with Norway spruce. Scots pine and other broadleaves are mainly located at low altitude, especially in the southern part of the study area.

In October 2018, the eastern Alps were hit by a severe windstorm coming from the Adriatic Sea, with south to north direction (Giovannini et al. 2021). The event, called Vaia, was characterized by extremely strong winds up to 200 km/h, and affected mainly the forests of the Eastern Italian Alps, including those of the study area, where it caused damage to 33.7 km^2 of forests (Giannetti et al. 2021).

3 Methods

In this study, remote sensing data were used to derive forest characteristics and consequently compute the forest wind vulnerability by using the semi-mechanistic Forest-GALES model. The spatially distributed parameters of the wind intensity-frequency distributions were derived from wind data provided by an ensemble of Convection-Permitting Models (CPMs) from the CORDEX-FPS project for both historical and future periods. Combining these two outcomes, the study classified the forest area into three different levels of risk. The three sections below report in detail the methodology and the data used.

3.1 Forest wind vulnerability

The procedure used by Baggio et al. (2026) was adopted to calculate and map the critical wind speeds (CWS). The methodology incorporates the semi-mechanistic model Forest-GALES for computing the CWS, directly deriving the input data of forest stand characteristics through the analysis of high-resolution remote sensing data. The routine developed by Baggio et al. (2026) is divided into two modules, and the necessary inputs are the CHM (Canopy Height Model) and a vector layer representing the forest species composition.

The first module processes the CHM to identify the position of individual trees and associates to each of them the species, crown radius, height, and Diameter at Breast Height (DBH, at 1.3 m height from the ground). The DBH is calculated from height-DBH relationships derived from local field survey data. The second module resamples the individual tree values in a 20×20 m raster grid, integrating the information of stand characteristics to calculate stand density, dominant height, distance to the forest edge, and the extent of the corresponding forest gap (if applicable). All these data are then reorganized in a single dataset and automatically passed to ForestGALES to calculate the CWS. For further information about the script that was implemented in the R language, we refer to the GitHub repository (https://github.com/TommBagg/CWS_calculation_fgr).

The CHM data for the area of this study were downloaded from the geoportal of the Veneto region (https://www.regione.veneto.it/web/agricoltura-e-foreste/chm-agordina). The CHM was derived from the LiDAR data acquired by an aerial survey for the whole study area (Fig. 1) in the summer of 2019, with a mean resolution of 45 points/m^2. The final grid resolution of the CHM is 0.5 m, sufficient for identifying individual trees (Pitkänen and Maltamo 2004) and extracting all the necessary parameters needed to run the two R

modules. The species distribution map is also necessary to run the first module. For this, a shapefile of the forest categories adopted at the regional scale for forest management was used. However, the forest classification adopted in this dataset adheres to Italian national legislation which can result in some areas with small groups of trees, especially at high altitude, to be excluded from the species mapping. To obviate this, we added a 200 m buffer to the species shapefile to assign a species to every tree detected from the CHM. The height of every tree was directly derived from the CHM, while the DBH was calculated within the same script by providing species-specific allometric height-DBH functions. These functions are reported in table SI-1, and they were derived from field surveys conducted between 2014 and 2024 (unpublished data collected by some of the authors and their research group) in forests within a maximum distance of 100 km from the study area. The best fitting relationships for the species investigated were polynomial of second order functions.

The output of the first module of the algorithm (Baggio et al. 2026) is a dataset where each point represents a tree with its relative characteristics. A thorough check of the location and quality of the dataset in a GIS environment highlighted that some points did not represent trees due to the low processing accuracy of the LiDAR data – i.e., treetops had been identified next to rock cliffs, on electric lines, cable yards systems of the ski resorts, and in urban areas. Therefore, we used the shapefile layer of the land use cover (freely available from the geoportal of the Veneto region, https://idt2.regione.veneto.it) to identify and remove the false positive treetops identified within urban and rocky areas. Similarly, we applied a 5 m buffer to the shapefile of the cable yard systems, the electricity lines, and the relative poles to further prevent spurious treetop identification.

The clean dataset was successively used as input for the second module to compute the forest stand characteristics and to consequently calculate the CWS with the ForestGALES model. ForestGALES (Hale et al. 2015) is a hybrid mechanistic, process-based wind risk model for the forestry sector. The latest version of the model (Locatelli et al. 2021) includes methods to compute wind risk metrics at both the stand-level and for individual trees within a stand. ForestGALES calculates the vulnerability of a tree or forest from tree and stand data (tree species, tree height, DBH, spacing between trees, soil type and rooting depth), and landscape information, i.e., the size of upwind forest gaps and their location relative to the tree/forest. Vulnerability is expressed as the two CWSs of damage calculated for stem breakage and overturning. In the ForestGALES simulation, soil conditions were assumed to be unfrozen, as commonly adopted in the standard model parameterization used for regional wind-risk mapping (Gardiner et al. 2024). In this study we did not take into account any future changes in forest conditions, so the characteristics and species distribution of the forest area, and the same map of CWS were used for both the present and future time periods. The account for the change of forest cover (in terms of species composition and forest metrics) for the future scenario is not addressed in this study, and we focuses on the impact of climate change on winds alone and analyzes the possible change of forest wind risk under historical and future climate conditions by keeping the same current forest.

3.2 Climate data and statistical analysis

Wind data are derived from an ensemble of 7 CPMs produced by the CORDEX Flagship Pilot Study project on Convective Phenomena over Europe and the Mediterranean (CORDEX-FPSCONV; Coppola et al. 2020) and available at the time of this study (Table

SI-2). All CPMs, except MOHC, are nested in a European-wide RCM (Regional Climate Model) and cover the greater Alpine region for two 10-year time slices: 1996–2005 for the historical period and 2090–2099 for the future under the Representative Concentration Pathway (RCP) scenario RCP8.5. Previous studies proved the ability of the ensemble in the representation of several atmospheric fields, including wind, and the reduction of uncertainty compared to the driving RCMs (Fosser et al. 2024; Belušić and Lind 2025). Since the CPMs have different spatial resolutions, ranging from 2.2 to 3 km, a first-order conservative remapping was applied to a regular grid of ~3 km spatial resolution in order to compare them on equal terms (Jones 1999).

We analyzed the most intense wind direction using historical observation data of the weather stations within the study area (managed by ARPAV, Veneto agency for environmental protection and prevention, https://www.arpa.veneto.it/dati-ambientali/open-data/clima). We detected two predominant wind directions, from south to north (wind named "Scirocco") and from north to south ("Föhn"). For both wind directions, we derived the wind intensity frequency distribution for both the historical period and the future scenario. The extreme value analysis was performed for each CPM independently, and only subsequently the ensemble mean was calculated.

We adopted the Gumbel extreme value distribution to calculate the frequency intensity curve. First, the maximum yearly wind intensity was extracted from the hourly timeseries for the south (pointing SW, S, and SE) and north (pointing NW, N, and NE) direction for each grid point. Then, we derived the parameters of the cumulative distribution function (Eq. 1), named β (location) and μ (scale).

$$F(x) = e^{-e^{-(x-\mu)/\beta}} \tag{1}$$

By using the two parameters of the Gumbel distribution, we derived the wind speed for the 30-, 50- and 100-year return periods at each grid point of the investigation domain. Then, the ensemble mean was calculated by averaging the expected wind intensities computed from each CPM independently. For each return period and scenario, the final data are 3 km gridded maps of hourly mean wind speed for the two predominant wind directions.

3.3 Forest wind risk

Forest wind risk is the combination of forest vulnerability and the probability of occurrence of a certain windstorm event. These two datasets are spatially explicit, but the wind intensities for the different return periods are at a coarser resolution compared to the CWS. Therefore, the former are resampled (bicubic method, "terra" package), to the final resolution of 20 m to match that of the CWS. Moreover, to account for the effect of the fine orography, a DTM (Digital Terrain Model) at 20 m resolution is used to derive the TOPEX index, which represents the degree of shelter of a given location based on a DTM and the distance from the observation point. Confidence in this approach was high as a similar approach of coupling the TOPEX index and wind intensity with ForestGALES wind risk calculations had been previously successfully used and validated in a small dolomitic area by Costa et al. (2023). Therefore, we adjusted the wind intensities according to the TOPEX index, consequently decreasing the wind speed of sheltered locations and keeping the raw values for completely wind-exposed locations. Equation 2a and 2b report the relations to

account for the sheltering effect of the orography in accordance with the two analyzed wind directions (*n* and *s* in Eq. 2a and 2b stand for northward and southward direction, respectively). The TOPEX index was increased by a unit to allow the scaling of the wind intensity ($Wn_{int,cor}$ and $Ws_{int,cor}$), therefore completely sheltered areas have a TOPEX value of 1, and exposed areas of 0.

$$Wn_{int,cor} = \frac{Wn_{int}}{TOPEXn + 1} \tag{2a}$$

$$Ws_{int,cor} = \frac{Ws_{int}}{TOPEXs + 1} \tag{2b}$$

We then combined the CWS and the expected wind intensities with a logistic damage probability function to calculate wind risk. This approach directly compares a value of predicted wind speed with the calculated CWS from the ForestGALES – fgr model. Equation 3 reports the logistic function, where *S* is a slope factor that was set to 6, as in (Chen et al. 2018). WS_{RT} refers to the wind intensity extracted for a given return period as described in Sect. 3.2 and corrected for the orographic shelterness (Eq. 2a and 2b).

$$P\,(damage) = \frac{1}{1 + e^{-\frac{WS_{RT} - CWS}{S}}} - \frac{1}{1 + e^{-\frac{CWS}{S}}} \tag{3}$$

The relation is commonly adopted for assessing the occurrence probability of an event between 0 and 1 in a smooth sigmoid shape. Similar logistic functions were used in previous wind damage analyses. Gardiner et al. (2024) used a version of Eq. 3 to back-calculate the probability of wind damage of tree along railway lines, using a damage threshold of 0.5. For this study, the same threshold value was used for classifying the forest area into three classes of risk according to three return periods of wind intensities, equal to 30, 50 and 100 years. These years correspond to the classes of high, medium, and low risk, respectively (Table 1). These classes are inspired by the classification used for mapping gravitational hazards. Since the wind data are produced for two wind directions (north to south and vice versa) for the two scenarios (historical and future) two different forest risk maps are produced. In this study, the two maps of the same scenario for the two wind directions are merged together by keeping the highest risk value for every raster cell.

To quantitatively analyze the distribution of the wind forest risk, the final hazard map was intersected with the shapefile of forest types. In this way, the area of each forest type was classified in one of the three risk classes, thus highlighting the stands at higher risk and providing the proportions of area at the different risk levels. To quantify the biomass at risk, we calculated the standing biomass volume for forest types per class of risk level. The calculation of the volume is based on the single tree calculations, since the dataset for deriving the CWS incorporates the position of every single tree associated with its height and DBH.

Table 1 Matrix of the wind forest risk

	Average hourly wind intensity Return Period		
	30 y	50 y	100 y
Forest damage *P(damage) > 0.5*	**HIGH**	**MEDIUM**	**LOW**

Equation 4a and 4b were adopted to calculate the tree stem volume of broadleaves (V_b, Bouvard (1938) and conifers (V_c, Algan (1981).

$$V_b = \frac{DBH^{2} * H}{2} \tag{4a}$$

$$V_c = \frac{DBH^{2} * H}{3} \tag{4b}$$

4 Results

4.1 Critical wind speeds

The first result of the study is the CWS computed with ForestGALES, by adopting the Turning Moment Coefficient method, which incorporates forest characteristics both at the single tree and stand level. ForestGALES calculate the CWS of overturning and stem breakage, and we selected the lower values among them to describe the most critical conditions for forest vulnerability. The output of ForestGALES is CWS expressed as mean hourly wind speed to match with standard climatological wind data, (Locatelli et al. 2021) and for this reason some forest areas can have really low values (e.g. 5 m/s). In Fig. 2, we report the

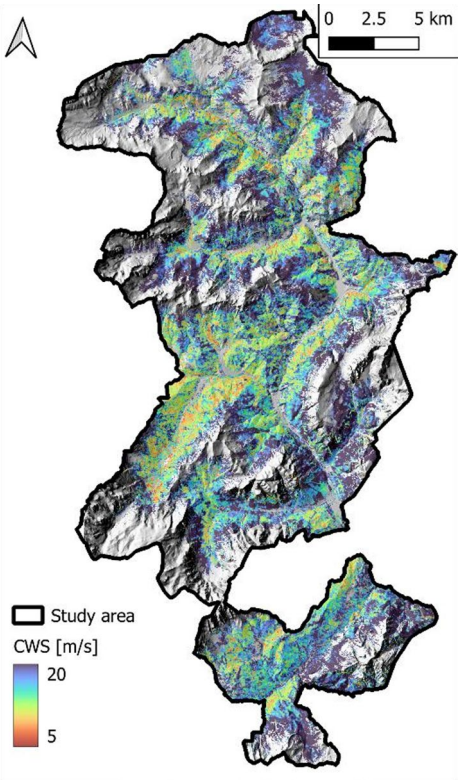

Fig. 2 Map of critical wind speed (CWS) of the forest area, red colour indicates low CWS and hence higher vulnerability. Dark blue indicates high CWS and hence low vulnerability

map of the CWS for the area of interest, where low values indicate forests more prone to wind damage (meaning that even less intense winds can damage such forests, colored in red), while higher values indicate less vulnerable forests and trees (colored in blue). Most of the southern parts of the domain are at low vulnerability, compared to the north, mainly for the presence of more broadleaves (due to the lower altitude) and the limited height of the stands. In the central and northern parts, the forest stands are more vulnerable toward the valley bottom due to the predominance of Norway spruce. Near the ridge lines, and thus at higher altitude, the presence of European larch, a species quite resistant to wind disturbances, decreases the vulnerability of those zones.

4.2 Wind climate mapping

The parameters β (location) and μ (scale) of the Gumbel extreme value distribution of the CPM data were calculated for the southward and northward wind directions and for the two reference periods. The maps of max expected hourly wind intensities together with the spatial mean and standard deviation are reported in Supplementary Information (Figures SI-1 to SI-12 and Table SI-3) for the two wind directions, the two reference periods and the three return periods. The wind intensity is expected to increase (increment of 0.13 m/s) for the return period equal to 30 years, while for higher return periods it is projected to increase between 0.27 and 0.34 m/s (~+3% increment) in the future compared to the historical period. However, such increments can be detected just for the wind direction from south to north, while the computed changes related to the opposite direction were negligible.

The TOPEX index is derived for both directions and is used to incorporate the orographic (shelter) effect on the wind intensity. The final maps of wind intensities were then produced for the three return periods necessary to define the risk levels as reported in Table 1. Figures SI-1 to SI-12 report the intensity of winds characterized by return periods of 30, 50 and 100 years in the historical and future period, together with the TOPEX index (panel B) and the final map of wind intensity including the orographic effect (panel C). By including TOPEX, it is possible to notice that the wind intensity is particularly high on the valley slope in the central part of the domain and in some areas in the northeast part, similarly to the findings of Schmoeckel and Kottmeier (2008). The difference in expected wind intensities between the two scenarios (including the TOPEX index) are reported in Figure SI-13, where areas with the greater increase in wind speed are shown.

4.3 Wind risk

Following the matrix reported in Table 1, the maps of forest wind risk were derived from the CWS and the wind intensity maps for both the two wind directions and the two reference periods. We merged the two risk maps representing the two wind directions of a reference period by keeping the highest risk value at each pixel. The two risk maps are reported in Fig. 3 for the historical and the future periods, respectively, in panels A and B. Panel C shows the difference in terms of new, stable and declining risk from the historical to the future scenario for a portion of the computational area. Maps in Fig. 3A and B are the combination of wind forest vulnerability (CWS) and wind intensity that are reported in Fig. 2 and Figures SI-1 to SI-12, respectively. The final risk maps highlight the areas at high, medium, and low levels of wind risk. In Fig. 3, two major areas at high risk in the historical

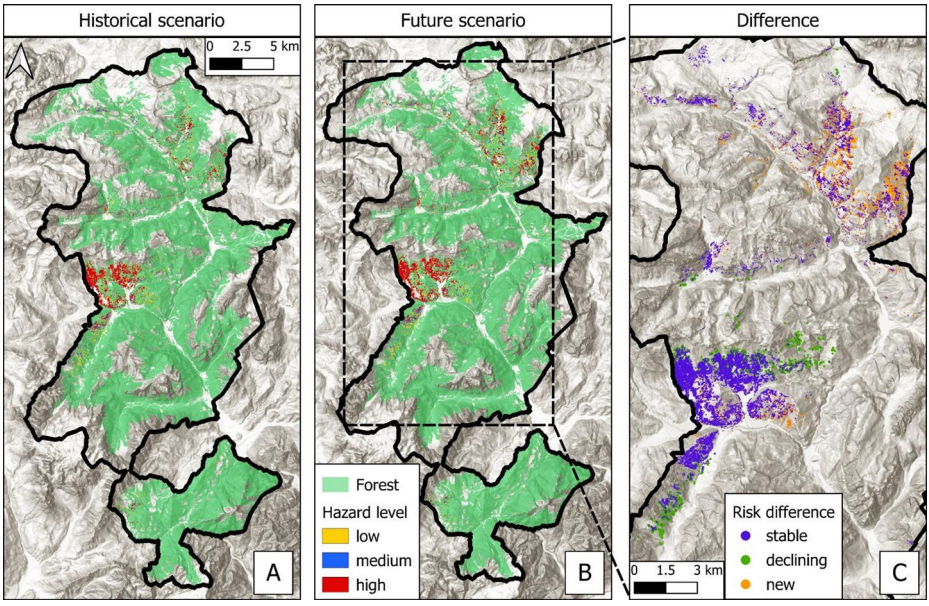

Fig. 3 Risk maps of forest wind disturbance for the historical (**A**), future (**B**) scenarios and difference of risk between the two reference periods (**C**)

period can be identified: a large area in the central part of the investigation domain, and a smaller one in the north-east. Comparing the historical and the future scenarios, it is possible to detect differences in the number and extent of areas exposed to a given level of risk. In the future scenario, the forest areas at high risk are increasing in terms of extent, mainly by buffering the areas at risk identified in the historical period.

To investigate the distribution of the risk levels by forest type, we extracted the pixel values of risk and by associating the related forest category, we derived the chart reported in Fig. 4 and the values in Table 2. Of the 26,812 ha covered by forest in the investigation area (Table 2), 1423 ha (5.31% of the total forest surface) belonged to one of the three classes of risk in the historical period. In the future period, the area exposed to any level of risk is projected to increase, reaching 6.36% of the total area, equivalent to 1704 ha.

The share of forest category in Table 2 indicates that most of the forest area is covered by stands of either Norway spruce (37%) or a mix of larch and Swiss stone pine (32%). In the historical period, the stands of Norway spruce are located in one of the three risk classes for 11.5% of their relative area, against 1.36% of the larch and Swiss stone pine stands. These values are projected to increase to 13.37 and 2.21% respectively by the end of the century. In the future period, forests composed of a mix of Norway spruce and beech will be exposed to risk for 8.20% of their relative area, against 7.41% of the historical period. Beech, Scots pine, and other broadleaves (including stands of Oak, Carpinus and Fraxinus) show the lowest values of relative areas exposed to risk, respectively equal to 0.13, 1.06 and 0.57% for the time period 1996–2005, with just the latter two showing a slight increase for the future period. Instead, for the beech forests, the area at any risk level remains constant. The forest area covered by Green alder and Mountain pine is equal to 2193 ha (8% of the forest area). In such areas, it is frequent to find single or small groups of trees, mainly of

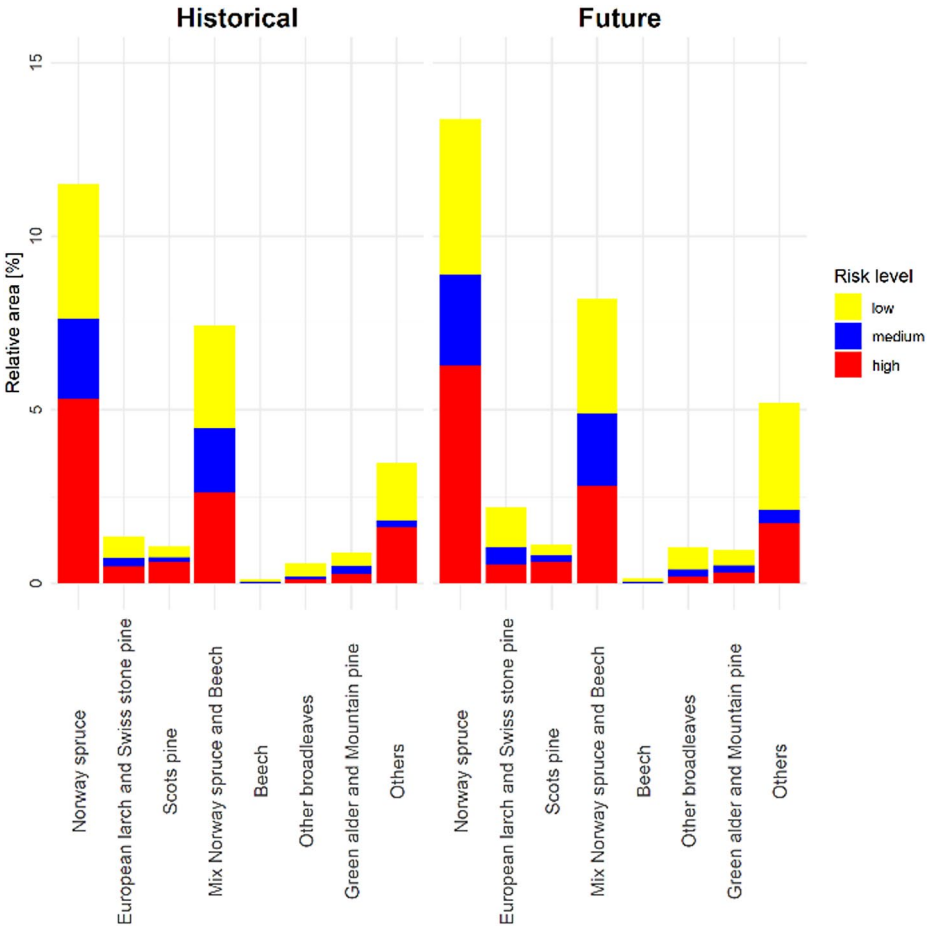

Fig. 4 Level of risk per forest stand category for historical and future scenarios. Data reported are percentages of the total forest area within the computational domain

Norway spruce, and therefore the trees identified within the "Green alder and Mountain" forest category were assigned to the Norway spruce species for the calculation of the forest wind vulnerability. However, here we plot them separately because the characteristics of the forest stand are rather different from the stands of pure Norway spruce. Indeed, the area exposed to a certain level of risk is equal to 0.88% and 0.96% in the historical and future periods, respectively. The overall characteristics of the trees classified at risk, divided into the two scenarios, are reported in Figure SI-14. The high risk category is mostly comprised of tall, even-aged stands located at quite high altitude (average of 1418 m a.s.l.) and on inclined slopes (average of 32.9°). These environmental characteristics clearly indicate the main protective function of these forests against the risk of natural hazards such as rockfalls, snow avalanches and shallow landslides.

From Fig. 4 it is notable that the total area of forest areas at high level of risk is larger than those at medium and low risk, implying that a windstorm event characterized by an intensity of 30 years return period might produce severe and extensive damage. This is

Table 2 quantitative assessment of forests into cumulative risk (combining high, medium and low risk classes) per forest category and for the historical and future scenarios

Stand category	Area [ha]	Risk area [ha] historical	Risk area [ha] future	Risk [%] historical	Risk [%] future	Risk increase [%]
Norway spruce	9915.4	1140.0	1325.7	11.50	13.37	16.29
European larch and Swiss stone pine	8706.0	118.7	192.6	1.36	2.21	62.26
Scots pine	541.0	5.8	6.0	1.06	1.12	3.45
Mix Norway spruce and beech	1694.2	125.6	139.0	7.41	8.20	10.67
Beech	2757.5	3.7	3.7	0.13	0.13	0.00
Other broadleaves	869.4	4.9	8.9	0.57	1.03	81.63
Green alder and Mountain pine	2192.8	19.3	21.0	0.88	0.96	8.81
Others	135.3	4.7	7.0	3.46	5.20	48.94
TOTAL	26811.6	1422.6	1704.0	5.31	6.36	19.78

especially true for the pure Norway spruce stands, which are the most abundant forest type within the domain.

4.4 Growing stock at risk

To better assess the impact of present and future windstorms on the forest areas, the standing volume of the trees falling in any class of risk was calculated and is shown in Fig. 5. The total volume of biomass at risk increases from 316,000 m^3 to 373,000 m^3, equal to 8.45 and 9.95% forest stocks, in the historical and the future scenario, respectively. The increase in relative terms of the growing stock at risk is equal to 17.77%. Similarly to the data reported in Table 1, the forest type that is increasing the most the volume at risk is pure Norway spruce (increase of 36,000, i.e. 14.48%). The stands of European larch and Swiss stone pine stands, and mixed Norway spruce and beech stands are projected to increase by ~ 15,000 m^3 and 3,600 m^3, respectively. However, in relative terms, the forest type whose growing stock is projected to have the largest increase is the European larch and Swiss stone pine, with + 62.94%. Beech forests instead show an almost constant value of volume at risk between the two scenarios.

5 Discussion and conclusions

This study provides a high-resolution quantitative assessment of the forest wind risk in a large forested area in the Belluno province in the Eastern Italian Alps, by integrating both forest characteristics and projected wind intensities under historical and future climate conditions (reference periods: 1996–2006 and 2090–2099 respectively). The innovative approach of the study stands in the use of high-resolution mapping of forest wind vulnerability (calculation of the critical wind speeds) together with the use of CPM for deriving the frequency intensity relationship of wind speed. The study maps for the first time the forest wind risk in an alpine context, by classifying the forest area into three different classes of risk (high, medium, low) at a fine resolution scale of 20 × 20 m. The critical wind speed map (Fig. 2) were calculated with a procedure that incorporates stand and tree characteris-

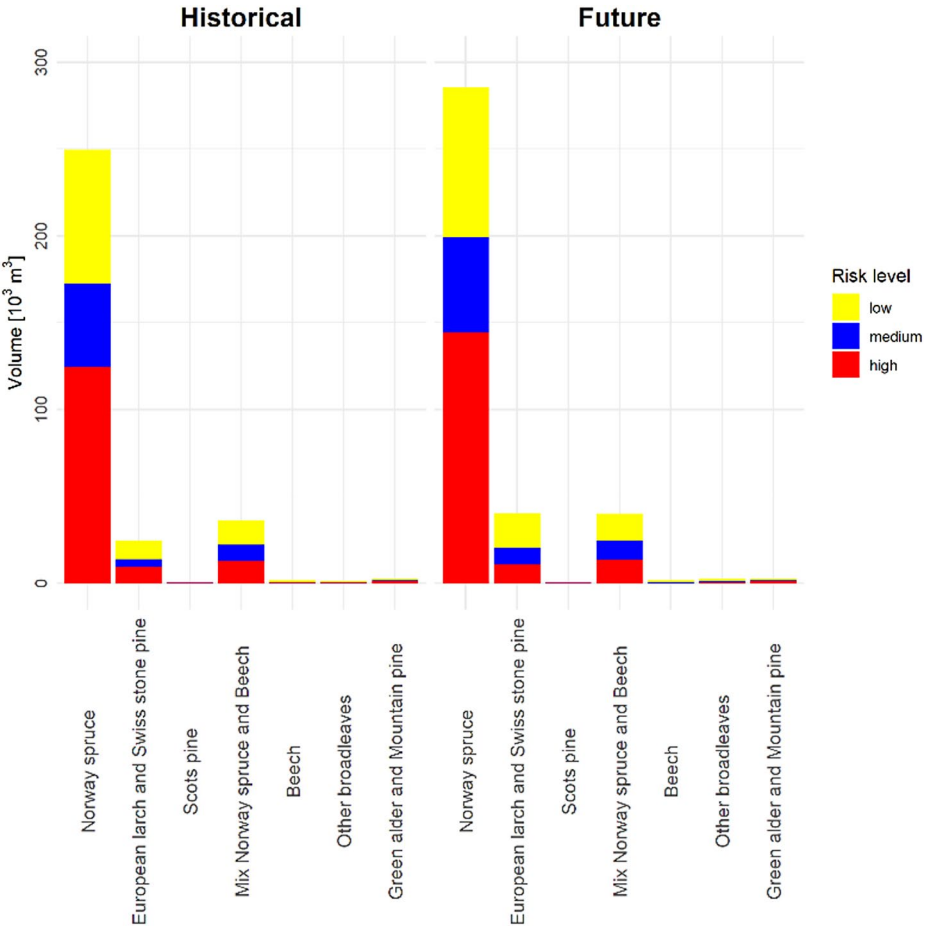

Fig. 5 Standing volume of trees at risk for the historical and future scenarios

tics that influence forest stability (tree height, DBH, stocking density, species composition, crown area, dominant height, distance to and extension of upwind gaps (Quine et al. 2021; Gardiner 2021), improving the approaches adopted in previous studies (Szymczak et al. 2022; Pawlik and Harrison 2022; Gardiner et al. 2024). In particular, this study precisely maps the risk of forest wind damage in terms of area extent and standing volume, deriving these metrics from calculation at the single tree level. This high resolution mapping allows identifying also small patches (<1 ha) in the high risk class that are of key importance in the alpine region context (Senf and Seidl 2020). Moreover, This is of particular importance in light of the expected of an increase in the frequency of wind disturbance in such small areas under climate change, as shown in Fig. 3, and in accordance with previous results by Senf and Seidl (2021).

CPM data allow obtaining reliable wind intensities at high spatial resolution, a fundamental requirement given the complex orography of the study area (Belušić Vozila et al. 2024). The CPM wind intensities calculated in this study indicate a mean increase of about 0.30 m/s by the end of the century compared to the historical, which results in greater increases up to

3% for high return period events (100 years, i.e. the most severe). As expected, the projected increase in mean wind velocities further increases the forest area at risk. To further improve the accuracy and reliability of the projected wind speed, the spatial resolution of these data could be increased. In our study we adopted the TOPEX index (frequently used in wind studies) to account for the impact of the complex alpine topography. Improvements of CPM resolution outputs can be derived by statistically downscaling the CPM outputs to sub-km scale. However, the statistical approach can relatively easily downscale the CPM outputs, but without appropriately taking into account the physics at the microscale level.

Our wind forest risk analysis shows that, in the historical period, the area in any of the three classes of risk results equal to 1422 ha, equivalent to 5.31% of the forest area, while the endangered area is projected to increase to 1704 ha (equivalent to 6.36%) under the RCP 8.5 scenario considering only the climate change impacts on the wind hazard alone. As highlighted by the boxplots in Figure SI-14, the trees classified at risk in the future scenario show a slight decrease in their wind vulnerability (higher values of CWS) but are associated with substantially higher values of expected wind speed (especially for the return period of 100 years). This means that the increased wind risk in the future scenario is mainly driven by the expected increase in wind intensities, especially in the northeast zone of the computational area (Figure SI-13). It is noteworthy that our analysis is based on the post-storm forest conditions after the occurrence of the storm Vaia in 2018 (forest conditions extracted from the LiDAR survey acquired in summer 2019). The storm Vaia came from the south (Adriatic sea) with a northward direction (Giovannini et al. 2021), and it generated wind gusts up to 200 km/h recorded by weather stations within the Cordevole catchment (Source: ARPAV, Environmental Agency of Veneto Region). It is therefore reasonable to expect that the forests that resisted such storm should be less vulnerable to storms under the actual forest characteristics. Regardless, the results of our study indicate that vulnerable areas are still present, and that climate change is likely to exacerbate the current risk. Similarly, Costa et al. (2023) reported that even if highly vulnerable trees were damaged by storm Vaia, the average forest wind vulnerability after Vaia remained almost equal to the pre-storm conditions in the Rocca Pietore municipality (part of the Cordevole catchment). With these post-storm conditions and the reported results, the study calls even more for urgent and effective forest management operations to mitigate the relative growing stock at risk.

The most exposed forest category is that of pure Norway spruce stands, with a percentage of area at risk equal to 11.50% and 13.37% for the historical and future scenarios, respectively. These high values can be attributed to both species-specific characteristics and exposure to one of the two prevailing wind directions – i.e. the geographical location of these stands. In addition, most of these stands are characterized by even-aged tall trees (Figure SI-14), a result of past forest management, a management strategy often associated with higher wind risk (Macdonald et al. 2010; Nevalainen 2017) – although other studies emphasize the role of local conditions (e.g. soil type) and management decisions over the rotation period (Hanewinkel et al. 2014). Our findings are consistent with previous research showing that Norway spruce is particularly susceptible to windthrow, mainly due to its shallow root system and the low DBH: height ratio (Panferov et al. 2011; Roessiger et al. 2020). When Norway spruce is mixed with beech (Table 2), the relative area exposed to risk decreases to 7.41% for the historical period and to 8.20% for the future scenario, indicating that mixed spruce forests can be managed effectively to decrease risk (Paul et al. 2019; Brandl et al. 2020). As observed in several European forests in the recent past (Köster et al.

2009; Mezei et al. 2014), in the investigation area, the bark beetle infestation due to the large amount of biomass on the ground caused by the storm Vaia in 2018 is likely to have further weakened the spruce stands. In such situation, infested trees are likely to suffer windblow at lower wind speeds (Seidl and Rammer 2017). The aforementioned aspect was not taken into account in the CWS calculation, since the effect of bark beetle infestation on tree stability is not accounted for in ForestGALES. Conversely, the low risk of European larch stands, even if located in most cases in wind-exposed areas (high elevation and mountain ridges), highlights the resistance of this forest species ascribable to the deep rooting system and the strong and flexible wood (Brandl et al. 2020; Kraus et al. 2022). The stands of beech and of Scots pine show almost no change in area at risk by the end of the century, indicating a low level of vulnerability that the increase in wind intensity is not able to convert to higher risk.

The calculation of growing stock exposed at risk allows the detection of volume losses in case of a severe storm. From our analysis, the Norway spruce stands are at the highest risk, for which the growing stock in any class of risk is equal to 250,000 m^3 and 286,000 m^3 in the historical and future period, respectively. Our growing stock analysis, although performed with a simple formula broadly valid for all conifers, can provide an estimation of the stock of carbon at risk in case of strong storms since the calculation is made through the sum of single tree volumes (Thürig et al. 2005; Zhu et al. 2012). However, the area and the volume of growing stock at risk also have significant implications for the protection against gravitational hazard, which is of fundamental importance in the Alpine context for protecting infrastructures and the safety of local communities (Teich et al. 2024; Stritih et al. 2024). Indeed, the growing stock plays an important role in the economic incomes for the municipalities and therefore in providing primary services to citizens living in these areas (Romagnoli et al. 2023).

In our study, the forest cover and characteristics are assumed to be constant between the historical period and future scenario, thus providing an understanding of the implications of future events in the case of forest characteristics and management similar to present conditions. However, future species composition, forest structure, and the effect of management practices will certainly modify the forest characteristics in the coming decades, hopefully decreasing the vulnerability of the forest stock and consequently the risk of wind damage. Studies incorporating dynamic vegetation modeling suggest that adaptive responses, such as species shifts and the occurrence of disturbances, can significantly change the future forest structure (Scherrer et al. 2020; Anselmetto et al. 2022) and have a consequent impact on the risk of wind damage. Future work should therefore integrate forest growth and succession models alongside climate projections to better capture these interactions (Mina et al. 2017). Further improvement can derive from the inclusion of frozen soil conditions for the calculation of wind vulnerability to better represent the risk of damage from tree overturning; temperature changes reflected in the CPM can be used to derive the probability of frozen soil conditions before a storm. In this study this aspect was not simulated for two reasons. Firstly, most of the extreme wind events in the region come from the South ("Scirocco" wind) which bring relatively mild temperatures even in winter; secondly, the available ForestGALES anchorage coefficients were typically derived in unfrozen soil conditions (Szymczak et al. 2022; Costa et al. 2023).

Our study underscores the urgency of adapting forest management strategies to increase forest resistance to imminent and future disturbance regimes, providing quantitative estimation and high-resolution mapping of forests exposed to wind risk. Increasing structural

and species diversity, particularly by promoting the wider adoption of more wind-resistant species such as European larch and beech, will enhance the overall forest resistance of the area. These proactive measures are essential to safeguard the ecosystem services provided by forests in a warm and increasingly disturbance-prone climate.

Supplementary Information The online version contains supplementary material available at https://doi.org/10.1007/s10584-026-04203-7.

Acknowledgements Tommaso Baggio, Giorgia Fosser and Emanuele Lingua were supported by the CARIPARO Foundation through the Excellence Grant 2021 to the "Resilience" Project. Tommaso Baggio and Emanuele Lingua were supported by the Interreg Alpine Space "MOSAIC" project. Giorgia Fosser's work was supported within the RETURN Extended Partnership and received funding from the European Union Next-GenerationEU (National Recovery and Resilience Plan – NRRP, Mission 4, Component 2, Investment 1.3—D.D. 1243 2/8/2022, PE0000005, CUP J33C22002840002).

Author contributions All authors contributed to the study conception and design. Material preparation, data collection and analysis were performed by Tommaso Baggio, Giorgia Fosser and Tommaso Locatelli. The first draft of the manuscript was written by Tommaso Baggio and all authors commented on previous versions of the manuscript. All authors read and approved the final manuscript.

Funding Open access funding provided by Università degli Studi di Padova within the CRUI-CARE Agreement.

Data availability Data will be made available on reasonable request to the corresponding author.

Declarations

Competing interests The authors have no relevant financial or non-financial interests to disclose.

References

Algan (1981) Tables de production et méthodes de cubage des résineux. Office National des Forêts (ONF), France

Ancelin P, Courbaud B, Fourcaud T (2004) Development of an individual tree-based mechanical model to predict wind damage within forest stands. Ecol Manage 203:101–121. https://doi.org/10.1016/j.foreco.2004.07.067

Anselmetto N, Sibona EM, Meloni F et al (2022) Land Use Modeling Predicts Divergent Patterns of Change Between Upper and Lower Elevations in a Subalpine Watershed of the Alps. Ecosystems 25:1295–1310. https://doi.org/10.1007/s10021-021-00716-7

Baggio T, Costa M, Marchi N et al (2026) Improve the estimation of forest wind vulnerability through remote sensed data: a new methodology. Environ Model Softw 197:106825. https://doi.org/10.1016/j.envsoft.2025.106825

Belušić D, Lind P (2025) Benefits of kilometer-scale climate modeling for winds in complex terrain: strong versus weak winds. Weather Clim Dyn 6:863–877. https://doi.org/10.5194/wcd-6-863-2025

Belušić Vozila A, Belušić D, Telišman Prtenjak M et al (2024) Evaluation of the near-surface wind field over the Adriatic region: local wind characteristics in the convection-permitting model ensemble. Clim Dyn 62:4617–4634. https://doi.org/10.1007/s00382-023-06703-z

Blennow K, Olofsson E (2008) The probability of wind damage in forestry under a changed wind climate. Clim Change 87:347–360. https://doi.org/10.1007/S10584-007-9290-Z/METRICS

Bouvard (1938) Étude sur le cubage des arbres feuillus. Annales de l'École Nationale des Eaux et Forêts. Nancy, France

Brandl S, Paul C, Knoke T, Falk W (2020) The influence of climate and management on survival probability for Germany's most important tree species. Ecol Manage 458:117652. https://doi.org/10.1016/J.FORECO.2019.117652

Chapman L (2000) Assessing topographic exposure. Meteorol Appl 7:335–340. https://doi.org/10.1017/S1350482700001729

Chen Y-Y, Gardiner B, Pasztor F et al (2018) Simulating damage for wind storms in the land surface model ORCHIDEE-CAN (revision 4262). Geosci Model Dev 11:771–791. https://doi.org/10.5194/gmd-11-771-2018

Coppola E, Sobolowski S, Pichelli E et al (2020) A first-of-its-kind multi-model convection permitting ensemble for investigating convective phenomena over Europe and the Mediterranean. Clim Dyn 55:3–34. https://doi.org/10.1007/s00382-018-4521-8

Costa M, Gardiner B, Locatelli T et al (2023) Evaluating wind damage vulnerability in the Alps: A new wind risk model parametrisation. Agric Meteorol 341. https://doi.org/10.1016/j.agrformet.2023.109660

Crozier MJ, Glade T (2005) Landslide hazard and risk: issues, concepts and approach. In: Landslide hazard and risk. pp 1–40

DeWalle DR, Buda AR, Fisher A (2003) Extreme Weather and Forest Management in the Mid-Atlantic Region of the United States. North J Appl For 20:61–70. https://doi.org/10.1093/njaf/20.2.61

Fassnacht FE, Mager C, Waser LT et al (2025) Forest practitioners' requirements for remote sensing-based canopy height, wood-volume, tree species, and disturbance products. Int J Res 98:233–252. https://doi.org/10.1093/FORESTRY/CPAE021

Finnigan JJ, Belcher SE (2004) Flow over a hill covered with a plant canopy. Q J R Meteorol Soc 130:1–29. https://doi.org/10.1256/QJ.02.177;WGROUP:STRING:PUBLICATION

Flesch TK, Wilson JD (1999) Wind and remnant tree sway in forest cutblocks. Agric Meteorol 93:229–242. https://doi.org/10.1016/S0168-1923(98)00112-9

Fosser G, Gaetani M, Kendon EJ et al (2024) Convection-permitting climate models offer more certain extreme rainfall projections. npj Clim Atmos Sci 7:51. https://doi.org/10.1038/s41612-024-00600-w

Gardiner B (2021) Wind damage to forests and trees: a review with an emphasis on planted and managed forests. J Res 26:248–266. https://doi.org/10.1080/13416979.2021.1940665

Gardiner B, Peltola H, Kellomäki S (2000) Comparison of two models for predicting the critical wind speeds required to damage coniferous trees. Ecol Modell 129:1–23. https://doi.org/10.1016/S0304-3800(00)00220-9

Gardiner B, Byrne K, Hale S et al (2008) A review of mechanistic modelling of wind damage risk to forests. Forestry 81:447–463. https://doi.org/10.1093/forestry/cpn022

Gardiner B, Lorenz R, Hanewinkel M et al (2024) Predicting the risk of tree fall onto railway lines. Ecol Manage 553:121614. https://doi.org/10.1016/j.foreco.2023.121614

Giannetti F, Pecchi M, Travaglini D et al (2021) Estimating VAIA windstorm damaged forest area in Italy using time series sentinel-2 imagery and continuous change detection algorithms for 2021. 12:680. https://doi.org/10.3390/F12060680

Giovannini L, Davolio S, Zaramella M et al (2021) Multi-model convection-resolving simulations of the October 2018 Vaia storm over Northeastern Italy. Atmos Res 253:105455. https://doi.org/10.1016/j.atmosres.2021.105455

Hale SE, Gardiner B, Peace A et al (2015) Comparison and validation of three versions of a forest wind risk model. Environ Model Softw 68:27–41. https://doi.org/10.1016/j.envsoft.2015.01.016

Hanewinkel M, Kuhn T, Bugmann H et al (2014) Vulnerability of uneven-aged forests to storm damage. Forestry 87:525–534. https://doi.org/10.1093/forestry/cpu008

Jones PW (1999) First- and Second-Order Conservative Remapping Schemes for Grids in Spherical Coordinates. Mon Weather Rev 127:2204–2210. https://doi.org/10.1175/1520-0493(1999)127%3C2204:FASOCR%3E2.0.CO;2

Kaimal JC, Finnigan JJ (1994) Atmospheric boundary layer flows: their structure and measurement. Atmos Bound Layer Flows. https://doi.org/10.1093/OSO/9780195062397.001.0001

Kamimura K, Shiraishi N (2007) A review of strategies for wind damage assessment in Japanese forests. J Res 12:162–176. https://doi.org/10.1007/s10310-007-0005-0

Kamimura K, Gardiner BA, Koga S (2017) Observations and predictions of wind damage to Larix kaempferi trees following thinning at an early growth stage. Int J Res 90:530–540. https://doi.org/10.1093/forestry/cpx006
Köster K, Voolma K, Jõgiste K et al (2009) Assessment of tree mortality after windthrow using photo-derived data. In: Annales Botanici Fennici. pp 291–298
Kraus D, Wohlgemuth T, Castellnou M, Conedera M (2022) Disturbance Ecology. Springer International Publishing, Cham
Locatelli T, Tarantola S, Gardiner B, Patenaude G (2017) Variance-based sensitivity analysis of a wind risk model - Model behaviour and lessons for forest modelling. Environ Model Softw 87:84–109. https://doi.org/10.1016/j.envsoft.2016.10.010
Locatelli T, Gardiner B, Hale S, Nicoll B (2021) fgr: r Version of the ForestGALES wind risk model. R package version 1.0
Macdonald E, Gardiner B, Mason W (2010) The effects of transformation of even-aged stands to continuous cover forestry on conifer log quality and wood properties in the UK. Int J Res 83:1–16. https://doi.org/10.1093/FORESTRY/CPP023
Mezei P, Grodzki W, Blaženec M, Jakuš R (2014) Factors influencing the wind–bark beetles' disturbance system in the course of an Ips typographus outbreak in the Tatra Mountains. Ecol Manage 312:67–77. https://doi.org/10.1016/j.foreco.2013.10.020
Mina M, Bugmann H, Cordonnier T et al (2017) Future ecosystem services from European mountain forests under climate change. J Appl Ecol 54:389–401. https://doi.org/10.1111/1365-2664.12772
Mortensen NG, Landberg L, Rathmann O et al (1999) Wind atlas analysis and application program (WAsP). orbit.dtu.dk
Nevalainen S (2017) Comparison of damage risks in even- and uneven-aged forestry in Finland. Silva Fenn 51:1–28. https://doi.org/10.14214/sf.1741
Outten S, Sobolowski S (2021) Extreme wind projections over Europe from the Euro-CORDEX regional climate models. Weather Clim Extrem 33:100363. https://doi.org/10.1016/j.wace.2021.100363
Panferov O, Sogachev A, Ahrends B (2011) Changes of Forest Stands Vulnerability to Future Wind Damage Resulting from Different Management Methods. Open Geogr J 3:80–90. https://doi.org/10.2174/1874923201003010080
Patacca M, Lindner M, Lucas-Borja ME et al (2023) Significant increase in natural disturbance impacts on European forests since 1950. Glob Chang Biol 29:1359–1376. https://doi.org/10.1111/gcb.16531
Paul C, Brandl S, Friedrich S et al (2019) Climate change and mixed forests: how do altered survival probabilities impact economically desirable species proportions of Norway spruce and European beech? Ann Sci 76:1–15. https://doi.org/10.1007/S13595-018-0793-8/METRICS
Pawlik Ł, Harrison SP (2022) Modelling and prediction of wind damage in forest ecosystems of the Sudety Mountains, SW Poland. Sci Total Environ 815:151972. https://doi.org/10.1016/j.scitotenv.2021.151972
Peltola HM (2006) Mechanical stability of trees under static loads. Am J Bot 93:1501–1511. https://doi.org/10.3732/ajb.93.10.1501
Peltola H, Kellomäki S, Väisänen H, Ikonen VP (1999) A mechanistic model for assessing the risk of wind and snow damage to single trees and stands of Scots pine, Norway spruce, and birch. Can J Res 29:647–661. https://doi.org/10.1139/x99-029
Pitkänen J, Maltamo M (2004) Adaptive Methods for Individual Tree Detection on Airborne Laser Based Canopy Height Model. Int Arch 36:187–191
Quine CP, Gardiner BA, Moore J (2021) Wind disturbance in forests: The process of wind created gaps, tree overturning, and stem breakage. Plant Disturbance Ecology, 2nd edn. Elsevier, pp 117–184
Renn O (2008) Concepts of risk: An interdisciplinary review - Part 1: Disciplinary risk concepts. GAIA 17:50–66
Roessiger J, Kulla L, Sedliak M (2020) A high proportion of norway spruce in mixed stands increases probability of stand failure. Cent Eur J 66:218–226. https://doi.org/10.2478/FORJ-2020-0017
Rojas-Labanda C, González-Rouco F, García-Bustamante E et al (2023) Surface wind over Europe: Data and variability. Int J Climatol 43:134–156. https://doi.org/10.1002/JOC.7739
Romagnoli F, Cadei A, Costa M et al (2023) TAMM Review: Windstorm impacts on European forest-related systems: An interdisciplinary perspective. Ecol Manage 541:121048. https://doi.org/10.1016/j.foreco.2023.121048
Scherrer D, Vitasse Y, Guisan A et al (2020) Competition and demography rather than dispersal limitation slow down upward shifts of trees' upper elevation limits in the Alps. J Ecol 108:2416–2430. https://doi.org/10.1111/1365-2745.13451
Schmoeckel J, Kottmeier C (2008) Storm damage in the Black Forest caused by the winter storm Lothar-Part 1: Airborne damage assessment. Hazards Earth Syst Sci 8:795–803

Seidl R, Rammer W (2017) Climate change amplifies the interactions between wind and bark beetle disturbances in forest landscapes. Landsc Ecol 32:1485–1498. https://doi.org/10.1007/S10980-016-0396-4/FIGURES/4

Seidl R, Thom D, Kautz M et al (2017) Forest disturbances under climate change. Nat Clim Chang 7:395–402. https://doi.org/10.1038/NCLIMATE3303

Senf C, Seidl R (2020) Mapping the forest disturbance regimes of Europe. Nat Sustain 4:63–70. https://doi.org/10.1038/s41893-020-00609-y

Senf C, Seidl R (2021) Storm and fire disturbances in Europe: Distribution and trends. Glob Chang Biol 27:3605–3619. https://doi.org/10.1111/gcb.15679

Stritih A, Senf C, Marsoner T, Seidl R (2024) Mapping the natural disturbance risk to protective forests across the European Alps. J Environ Manage 366:121659. https://doi.org/10.1016/j.jenvman.2024.121659

Szymczak S, Bott F, Babeck P et al (2022) Estimating the hazard of tree fall along railway lines: a new GIS tool. Nat Hazards 112:2237–2258. https://doi.org/10.1007/s11069-022-05263-5

Teich M, Stritih A, Bottero A, Moos C (2024) Global change impacts on avalanche protective forests — current knowledge and future research directions. 553–561

Thürig E, Palosuo T, Bucher J, Kaufmann E (2005) The impact of windthrow on carbon sequestration in Switzerland: a model-based assessment. Ecol Manage 210:337–350. https://doi.org/10.1016/J.FORECO.2005.02.030

Zhu K, Woodall CW, Clark JS (2012) Failure to migrate: lack of tree range expansion in response to climate change. Glob Chang Biol 18:1042–1052. https://doi.org/10.1111/j.1365-2486.2011.02571.x

Authors and Affiliations

Tommaso Baggio[1] · Giorgia Fosser[2] · Tommaso Locatelli[3] · Emanuele Lingua[1,4]

✉ Tommaso Baggio
tommaso.baggio@unipd.it

[1] TESAF Department, University of Padova, Viale dell'Università 16, 35020 Legnaro, Italy

[2] University School for Advanced Studies-IUSS Pavia, Piazza della Vittoria, 15, 27100 Pavia, Italy

[3] Forest Research, Northern Research Station, Bush Estate, Roslin EH25 9SY, Scotland, UK

[4] Research Center on Climate Change Impacts, University of Padova, Rovigo, Italy